Quaternary Research 77 (2012) 273–280

Contents lists available at SciVerse ScienceDirect

Quaternary Research

journal homepage: www.elsevier.com/locate/yqres

The deglacial history of NW Alexander Island, Antarctica, from surface exposure dating

Joanne S. Johnson [a,*], Jeremy D. Everest [b], Philip T. Leat [a], Nicholas R. Golledge [b,c], Dylan H. Rood [d], Finlay M. Stuart [e]

[a] British Antarctic Survey, High Cross, Madingley Road, Cambridge CB3 0ET, UK
[b] British Geological Survey, Murchison House, West Mains Road, Edinburgh, EH9 3LA, UK
[c] Antarctic Research Centre, Victoria University of Wellington, Kelburn Parade, Wellington 6140, New Zealand
[d] Lawrence Livermore National Laboratory, Center for Accelerator Mass Spectrometry, 7000 East Avenue, Livermore, CA 94550-9234, USA
[e] Scottish Universities Environmental Research Centre, Rankine Avenue, Scottish Enterprise Technology Park, East Kilbride G75 0QF, UK

ARTICLE INFO

Article history:
Received 3 June 2011
Available online 2 January 2012

Keywords:
Cosmogenic nuclides
Erratics
Ice sheet
Refugia
Wilkins Ice Shelf
Last glacial maximum

ABSTRACT

Recent changes along the margins of the Antarctic Peninsula, such as the collapse of the Wilkins Ice Shelf, have highlighted the effects of climatic warming on the Antarctic Peninsula Ice Sheet (APIS). However, such changes must be viewed in a long-term (millennial-scale) context if we are to understand their significance for future stability of the Antarctic ice sheets. To address this, we present nine new cosmogenic ^{10}Be exposure ages from sites on NW Alexander Island and Rothschild Island (adjacent to the Wilkins Ice Shelf) that provide constraints on the timing of thinning of the Alexander Island ice cap since the last glacial maximum. All but one of the ^{10}Be ages are in the range 10.2–21.7 ka, showing a general trend of progressive ice-sheet thinning since at least 22 ka until 10 ka. The data also provide a minimum estimate (490 m) for ice-cap thickness on NW Alexander Island at the last glacial maximum. Cosmogenic ^{3}He ages from a rare occurrence of mantle xenoliths on Rothschild Island yield variable ages up to 46 ka, probably reflecting exhumation by periglacial processes.

Introduction

Records of past changes in the Antarctic ice sheets are important for testing the reliability of ice-sheet models that will be used to predict the magnitude of future sea-level change, and for identifying forcing mechanisms for ice-sheet change. During the past decade, much work has been focused on increasing the spatial and temporal range of observations of past ice-sheet behavior from the terrestrial paleo-record of the Antarctic Peninsula (e.g., Bentley et al., 2006; Hodgson et al., 2009; Johnson et al., 2009; Bentley et al., 2011; Johnson et al., 2011). Despite these studies, the configuration of the Antarctic Peninsula Ice Sheet (APIS) and its rate of thinning since the last glacial maximum (LGM) are still not well-known. More observational data are required if we are to understand the long-term significance of recent changes including rapid thinning and acceleration of glaciers, and ice-shelf collapses (e.g. Cook et al., 2005; Hodgson et al., 2006; Pritchard et al., 2009).

During the past few decades, surface exposure dating using cosmogenic nuclides has rapidly complemented radiocarbon for dating geomorphic surfaces and has revolutionized studies of Antarctic glacial chronologies (Sugden et al., 2006). Many of those studies have utilized the 'dipstick' approach (Stone et al., 2003) for determining the thinning history of ice sheets since the LGM. In this approach, glacially transported (erratic) cobbles are collected from sites at various elevations on a nunatak. In turn, an age versus elevation profile is determined using surface exposure dating on each of those erratics. Here, we use the same approach to provide new surface exposure ages that record the deglacial history of NW Alexander Island and Rothschild Island, both situated on the western side of the Antarctic Peninsula (Fig. 1a). Although several studies have focused on deglaciation of the eastern coast of Alexander Island since the LGM (Clapperton and Sugden, 1982; Bentley et al., 2005; Bentley et al., 2006; Smith et al., 2007; Hodgson et al., 2009; Roberts et al., 2009), no glacial chronological data from other parts of Alexander Island or its surrounding islands have yet been published.

Background

Alexander Island is a large glaciated island situated on the western side of the Antarctic Peninsula, and is presently separated from it by George VI Sound. George VI Ice Shelf occupies George VI Sound (Fig. 1a). The island is mostly ice-covered at the present day, with exposed nunataks, especially in the north, and a few ice-free areas, such as Ablation Point Massif on its eastern edge (Fig. 1b). Alexander Island glaciers flow westward into the Wilkins and Bach ice shelves (Fig. 1a) and eastward into George VI Ice Shelf. George VI Ice Shelf is also fed

* Corresponding author. Fax: +44 1223 362616.
E-mail address: jsj@bas.ac.uk (J.S. Johnson).

0033-5894/$ – see front matter © 2011 University of Washington. Published by Elsevier Inc. All rights reserved.
doi:10.1016/j.yqres.2011.11.012

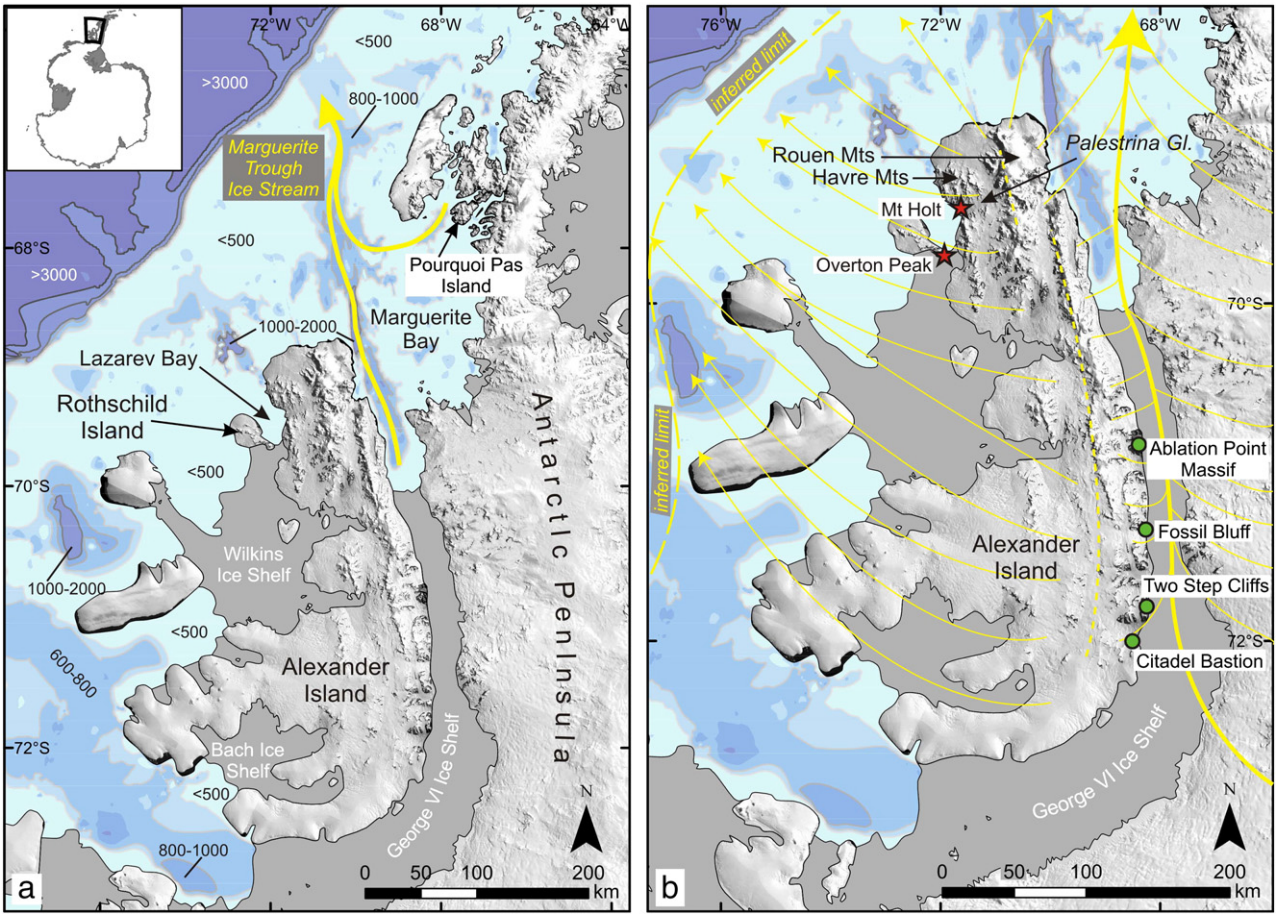

Figure 1. a. Map showing Alexander Island in relation to the southwestern Antarctic Peninsula (the inset shows the location in Antarctica). The satellite image is from Landsat Image Mosaic of Antarctica (LIMA). Bathymetry for Marguerite Bay is from GLOBEC (Bolmer, 2008), and for west of Alexander Island from Graham et al. (2010). Depths are shown in meters below sea level. b. Map showing our sample locations on Alexander Island and Rothschild Island (stars), and sites mentioned in the text (circles). Model flowlines from Clapperton and Sugden, 1982 (Fig. 9) are shown as yellow arrows; the ice divide is a dashed yellow line.

by glaciers from the Antarctic Peninsula. Rothschild Island is situated off the NW coast of Alexander Island (Fig. 1a). It is also predominantly ice-covered, but has a range of nunataks extending east–west across it, and a small glacier flowing into Lazarev Bay. The southern coast of Rothschild Island merges with the Wilkins Ice Shelf, which connects the island with Alexander Island to the east.

At the LGM, the APIS mostly extended to or close to the continental shelf edge (Sugden et al., 2006, Fig. 5). However, the details of its configuration at the LGM are still not well known and there are competing estimates for its thickness. A number of studies have inferred maximum paleo-ice thickness of more than 1 km at LGM from modelling (Denton et al., 1991; Huybrechts, 2002) and from terrestrial and marine geological data (e.g. Kennedy and Anderson, 1989; Bentley and Anderson, 1998). However, several ice-sheet reconstructions based on marine geological data suggest that the APIS was drained by ice streams extending close to the continental shelf edge (e.g., Larter and Cunningham, 1993; Anderson et al., 2002; Ó Cofaigh et al., 2005). These reconstructions imply that the APIS had a lower surface profile. Geomorphological observations support the presence of an ice cap on Alexander Island at the LGM (Clapperton and Sugden, 1982). The ice cap was initially separate from the APIS, but subsequently became confluent with APIS in George VI Sound. Clapperton and Sugden's reconstruction of the ice cap and flowlines is shown in Figure 1b. An early ice-sheet model (Payne et al., 1989) yielded an ice dome over Alexander Island which was over 3.5 km thick at LGM. Erratics were observed at 790 m a.s.l. on Ablation Point Massif (Fig. 1b; Clapperton and Sugden, 1982), indicating that ice was at least 800 m thick at this location. The other sites visited by Clapperton and Sugden (Fossil Bluff and Two Step Cliffs) appear to have been submerged by the LGM ice cap, leaving the authors unable to determine its maximum thickness. Surface exposure dates recently obtained from Two Step Cliffs indicate that the site only became ice-free in the early Holocene (7.4–8.4 ka: Bentley et al., 2006), implying that it was submerged by ice at the LGM. The maximum LGM thickness of the ice cap on Alexander Island therefore remains unknown. Peaks in the north of the island rise to nearly 3000 m a.s.l., as at Mt Paris and Mt Sanderson in the Rouen Mountains, which are 2700 and 2300 m a.s.l., respectively. These are potential sites for determining the maximum LGM thickness, but as yet their glacial history has not been studied. Evidence for rock outcrops on Alexander Island remaining ice-free at the LGM and through multiple glacial cycles is important for locating potential sites for biological refugia during glacial periods. It is thought that Alexander Island may harbor a biodiversity hotspot indicative of a glacial refuge, but any potential site is presently unknown (Convey et al., 2008).

Striated surfaces imply that ice drained from northern Alexander Island into Marguerite Bay (Fig. 1b; Clapperton and Sugden, 1982), for which we have a more complete deglacial chronology. Bathymetric data show that grounded ice extended to the continental shelf break west of Marguerite Bay at the LGM, and a large ice stream developed in Marguerite Trough (Fig. 1a; Ó Cofaigh et al., 2002). Ice retreated from the outer shelf around 13.0–14.2 cal ka BP (Pope and Anderson, 1992; Heroy and Anderson, 2007). This event was followed by rapid ice-stream retreat (Ó Cofaigh et al., 2005). Recently acquired surface exposure ages from Pourquoi Pas Island (Fig. 1a) imply that the rapid

https://doi.org/10.1016/j.yqres.2011.11.012 Published online by Cambridge University Press

retreat occurred around 10 ka (Bentley et al., 2011). An ice shelf formed in the mid-shelf region during this retreat, but then disintegrated before the inner shelf was deglaciated (Kilfeather et al., 2011).

Site description

We collected samples for surface exposure dating from two locations: Mount Holt, which is situated on NW Alexander Island, and an unnamed outcrop near Overton Peak on SE Rothschild Island (Fig. 1b).

Mount Holt, Alexander Island

Mount Holt forms a nunatak rising to ~750 m a.s.l. (Fig. 2a) from the middle of Palestrina Glacier, which drains westwards from the Havre Mountains into Lazarev Bay, on the NW coast of Alexander Island (Fig. 1b). The site was chosen for its position on a westward trending flowline in the LGM reconstruction of Clapperton and Sugden (1982) (Fig. 1b). Mt Holt is also directly downstream of an extensive area of granite outcrop around Care Heights and Golden Pass in the Rouen Mountains (Fig. 1b; Care, 1983), making it likely that granite erratics would have been deposited there when ice retreated. The peak is mostly composed of siliceous and calcareous metasedimentary rocks of the Mesozoic LeMay Group (Burn, 1984), and in places these have weathered to produce a thin cover of red/brown coarse gravelly regolith. On the inaccessible northern flank of the peak at ca. 400 m a.s.l. we observed ice-marginal landforms involving nested ridges aligned across the slope sub-parallel to the modern flow direction of Palestrina Glacier. An area of flat ground covers ca. 0.5 km^2 approximately 100 m above the ice-marginal landforms and about 250 m below the lee side, west of the summit. This area is formed by a bedrock ledge, draped with thin regolith.

Two granodioritic erratics (L7.1.1 and L7.1.2) were collected from a bedrock ledge at 580 m a.s.l. Both were well-rounded, and firmly embedded in the regolith cover. They also displayed marked differences in weathering between surfaces exposed above the regolith, where feldspars had weathered, leaving a pitted surface, and those protected beneath it, which retained a glacial polish. A third sample (L7.1.3) was taken 20 m below the summit at 729 m a.s.l. This was the only example of non-local lithology found at the locality, and the sample was comprised of amalgamated erratic sandstone pebbles, taken from a radius of 1 m within a ~30 m diameter flat area below the summit (Fig. 2a). The flat area had a thin drape of locally derived regolith, with sandstone erratics found in a small area at its edge.

Overton Peak, Rothschild Island

Rothschild Island is 45 km long and 24 km wide, and is dominated by several high, steep-sided hills forming a central NW–SE trending spine surrounded by ice piedmonts. Overton Peak is a prominent peak on the SE promontory of the island (Fig. 1b). Like the other steep-sided hills, Overton Peak consists of Mesozoic LeMay Group sedimentary rocks. There also are several outcrops of Cenozoic basaltic pyroclastic volcanic rocks on the island that form low, rounded hills. Our samples were collected from an un-named rounded hill consisting of basaltic scoria, which is located 2 km NW of Overton Peak (Fig. 2b). The hill is near the center of an ice dome which occupies much of SE Rothschild Island and rises to 296–318 m a.s.l. The site is well-placed to record ice flow from western Alexander Island across Lazarev Bay at the LGM. The samples were located on a relatively flat area covering 0.04 km^2, with a general slope of <10° to the north, and to the east on a hillside rising to a subdued summit at 660 m a.s.l. The surface formed by the basaltic rock is characterized by patterned ground and down-dip stripes on the flatter area (Figs. 2c and d), and poorly defined contour-parallel terraces on the steeper slopes. These features indicate that periglacial processes have been active at this site.

Our sample sites are underlain by unconsolidated basaltic scoria K–Ar dated at 5.4 ± 0.7 Ma (Smellie et al., 1988). The basalt contains abundant ultramafic xenoliths, with granitoid cobbles and boulders scattered over it (Fig. 2b). The xenoliths are commonly coated by glassy basaltic scoria, indicating eruption with the magma; this is never the case for the metasedimentary and granitoid clasts, indicating that the latter were deposited by a different process. Those were

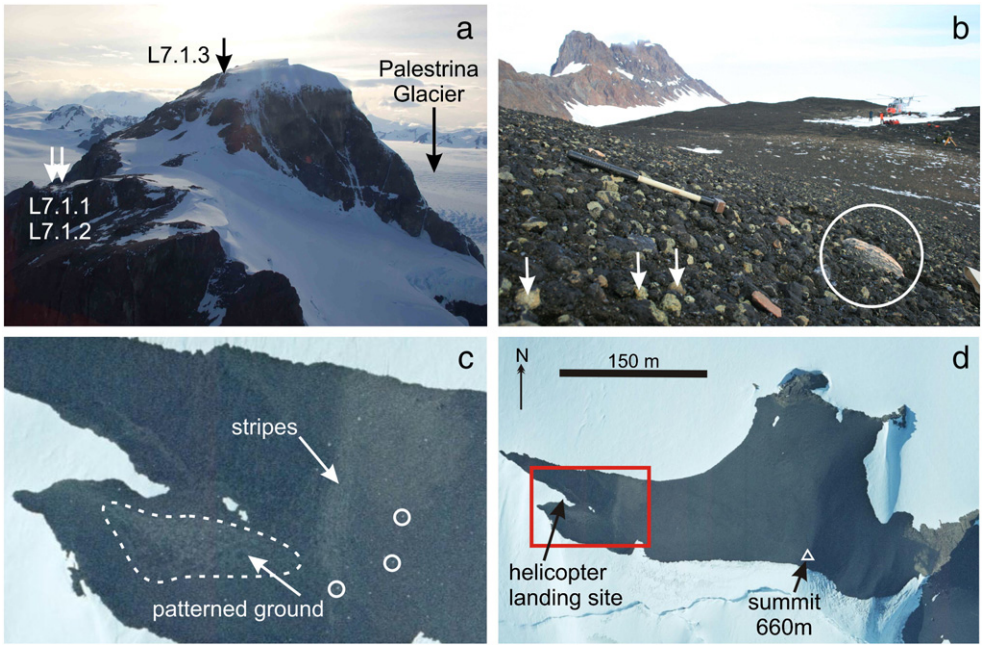

Figure 2. a. Photograph of Mt Holt looking NE. The cosmogenic sampling sites (arrows) are labelled; b. Photograph of site L7.201 at Overton Peak, looking west towards the helicopter landing site. The foreground is littered with mantle xenoliths (arrows) and several granitoid cobbles (circled) lie on the basaltic regolith; c. Aerial photograph of part of site L7.201 near Overton Peak (see Fig. 1b for location), showing evidence of periglacial processes, and numerous erratic cobbles strewn on the bedrock surface (examples are circled). The location of this image is shown in d; d. A large-scale aerial photograph of Overton Peak. The red box shows the location of c. Credit: Mapping and Geographic Information Centre, British Antarctic Survey.

https://doi.org/10.1016/j.yqres.2011.11.012 Published online by Cambridge University Press

most likely glacially transported from the extensive granite outcrops in northern Alexander Island (Care, 1983). We collected six granitoid erratic cobbles from 408 to 444 m a.s.l. Two samples (L7.201.2 and L7.201.3) were located in the flat, western part of the site, and samples L7.2.1 to L7.2.5 were from the eastern hillside, between the base and summit. Five ultramafic xenoliths were also collected from the base.

Methods

We collected samples for surface exposure dating from the sites described above. We sampled erratic cobbles in preference to bedrock to minimize the likelihood of obtaining anomalously old exposure ages due to nuclide inheritance (Bierman et al., 1999). We minimized the possibility of burial by snow by sampling at well-exposed localities, and collected samples from positions away from slopes or cliffs to minimize the possibility of post-depositional movement. Supporting evidence of glacial transport, such as striations, polish, and faceting, was also considered in sample selection. Erratics with evidence of severe weathering, involving deep pitting, flaking, or surrounding spalled debris, were avoided.

At all sites topographic shielding was measured and sample elevations were determined using handheld GPS set to reference coordinate system WGS84. Sample elevations at Overton Peak were later checked with photogrammetry from GPS-supported aerial photography with accuracy of ±1 m. Elevations were then corrected to meters above sea level. We also obtained the local ice surface elevation from the photogrammetry. We define this as the surface elevation of the present-day ice sheet immediately adjacent to our sample sites. However, we recognize that it is not straightforward to decide where to measure the local ice surface; for example, Mt Holt lies between two glaciers whose surface elevations decrease markedly seaward. Since we use our exposure ages to give minimum estimates for thickness of the LGM ice sheet, we chose an elevation from the upstream, rather than downstream, side of the nunatak. At Overton Peak, there is much less variation in surface elevation of the surrounding ice. Unfortunately we were unable to check our sample elevations at Mt Holt because there is no photogrammetry available for that region. However, we were able to extract the local ice-surface elevation with accuracy of approximately ±10 m from ASTER GDEM, which is a product of METI and NASA (http://www.gdem.aster.ersdac.or.jp/index.jsp). Details of all samples collected are given in Tables 1 and 2.

We analysed cosmogenic ^{10}Be in two granodiorite erratic cobbles from Mt Holt and six granitoid erratic cobbles from Overton Peak, as well as ^{10}Be in the amalgamated sandstone sample from Mt Holt. We also undertook cosmogenic ^{3}He exposure dating in four ultramafic xenoliths from Overton Peak (site L7.201). Measuring the abundance of cosmogenic nuclides ^{10}Be and ^{3}He normally provides minimum exposure ages. In a simple situation where an erratic was removed from previously unexposed bedrock or was eroded during transport within the ice, leaving no ^{10}Be from a previous exposure period remaining, the ^{10}Be concentration within it is directly correlated with the time elapsed since ice last retreated from the sample site. Cosmogenic ^{3}He does not radioactively decay and therefore records the total duration of exposure to cosmic radiation that a sample has ever experienced, not just that since the last retreat of ice. For this study, we chose to measure the abundance of ^{3}He in clinopyroxenes because the xenoliths do not contain quartz for ^{10}Be analysis.

Details of the analytical methods are given in the Supplementary data; sample information, ^{10}Be concentrations, calculated exposure ages and details of the scaling scheme used are given in Table 1. Exposure ages presented in Table 1 are calculated assuming zero erosion, and for comparison, assuming an erosion rate of 20 cm/myr. It is difficult to estimate an erosion rate for NW Alexander Island because there are no independent data available from anywhere on the Antarctic Peninsula. Erosion rates determined from elsewhere in Antarctica have been reported as typically very low (<10 cm/myr; Nishiizumi et al., 1991; Bruno et al., 1997; Summerfield et al., 1999). However, those studies are based on the Dry Valleys and Transantarctic Mountains which are much colder and drier than the Antarctic Peninsula, and would probably exhibit lower erosion rates. Because we do not know how much higher erosion rates are in our study area, we chose to apply a moderate erosion rate, 20 cm/myr, to our samples. This increases the exposure ages by less than 80 yr in all but one sample, L7.1.2, whose age increases by 500 yr (Table 1). Because the effect of erosion on our exposure ages is small, from here onwards we refer only to ages calculated assuming zero erosion. We report both internal and external uncertainties, but follow Balco et al. (2008) and use external uncertainties for our discussion because we compare our exposure ages with those from sites several hundred kilometers away.

Results

We obtained three ^{10}Be exposure ages from Mt Holt and six from Overton Peak, all on erratics (Table 1). If zero erosion is assumed, five with age range 10.2–15.7 ka postdate the LGM, and three fall within the LGM period that is here defined as occurring between ~19 and 26 ka (Clark et al., 2009). One age (54.4 ka; from Mt Holt) is

Table 1
^{10}Be concentrations and exposure ages.

Sample name	Latitude (deg. S)	Longitude (deg. W)	Elevation (m a.s.l.)	Thickness (cm)	Shielding correction[a]	^{10}Be (10^3 atoms/g)[b]	Standard	Exposure age (yr)[c]	1σ internal uncertainty (yr)	1σ external uncertainty (yr)	Exposure age with 20 cm/Ma erosion (yr)	1σ internal uncertainty (yr)	1σ external uncertainty (yr)
Mt Holt													
L7.1.1	69° 24.44′	71° 39.76′	580	5	0.990	153.2±3.6	07KNSTD	15,746	371	1422	15,787	373	1430
L7.1.2	69° 24.44′	71° 39.76′	580	4.5	0.990	526.1±8.6	07KNSTD	54,379	901	4872	54,868	918	4962
L7.1.3	69° 24.41′	71° 38.83′	729	4	0.999	246.1±6.0	07KNSTD	21,744	533	1972	21,822	537	1987
Overton Peak													
L7.201.2	69° 48.80′	72° 1.08′	411	5	0.998	164.4±3.8	07KNSTD	19,674	457	1777	19,737	460	1789
L7.201.3	69° 48.80′	72° 1.08′	411	5	0.995	115.8±2.7	07KNSTD	13,878	325	1252	13,910	326	1258
L7.2.1	69° 40.52′	72° 0.95′	408	5	0.995	174.0±4.1	07KNSTD	20,950	496	1895	21,022	500	1909
L7.2.2	69° 40.51′	72° 0.68′	444	5	0.995	91.7±2.2	07KNSTD	10,641	256	961	10,659	257	965
L7.2.4	69° 40.51′	72° 0.68′	443	4.5	0.995	101.1±2.0	07KNSTD	11,699	232	1045	11,721	233	1049
L7.2.5	69° 40.51′	72° 0.71′	439	5.5	0.995	87.4±2.1	07KNSTD	10,230	246	924	10,247	247	927

[a] Ratio of the production rate at the shielded site to that for a 2π surface at the same location calculated using the CRONUS-Earth Geometric Shielding Calculator Version 1.1.
[b] Calculated using 07KNSTD ^{10}Be measurement standard and calibration (Nishiizumi et al., 2007).
[c] Model exposure age assuming zero erosion, density 2.65 g/cm^3 and Antarctic atmosphere. This was calculated using the CRONUS-Earth ^{10}Be-^{26}Al exposure age calculator (Balco et al., 2008) Version 2.2, using a constant production rate model and scaling scheme for spallation of Lal (1991)/Stone (2000). Using the other main scaling factor schemes changes our exposure ages by only 2–7%.

https://doi.org/10.1016/j.yqres.2011.11.012 Published online by Cambridge University Press

Table 2
Helium isotope data and calculated exposure ages.

Sample	R/R_a crush	Melt weight (g)	^4He (10^{12} at/g)	$^3He/^4He$ (R/R_a)	$^3He_{cosmo}$ (10^6 at/g)	P_{local}[a] (at/g/yr)	Exposure age (yr)
L7.201.1.1	6.64 ± 0.04	0.320	2.26 ± 0.2	6.77 ± 0.16	0.66 ± 0.52	186	3,531 ± 2687
L7.201.1.4-1	6.51 ± 0.19	0.320	1.59 ± 0.02	9.43 ± 0.13	6.71 ± 0.54	186	35,907 ± 3891
L7.201.1.4-2	6.62 ± 0.06	0.432	1.06 ± 0.02	10.55 ± 0.11	6.16 ± 0.21	186	32,959 ± 2643
L7.201.1.12	6.53 ± 0.09	0.318	2.53 ± 0.03	7.53 ± 0.09	3.83 ± 0.38	186	20,492 ± 2.519
L7.201.1.25	6.62 ± 0.06	0.294	2.47 ± 0.03	6.59 ± 0.16	0.15 ± 0.59	186	803 ± 3157

[a] The local production rate (P_{local}) was calculated by scaling the global sea level high latitude cosmogenic ^3He production rate in pyroxene (124 ± 9.2 at/g/yr; Goehring et al., 2010) to the latitude and altitude of the sample site using factors of Lal(1991)/Stone(2000).

anomalously old. Whereas prior exposure and recycling from older deposits commonly result in anomalously old exposure ages, there are relatively few scenarios, such as snow cover or delayed emergence from deep within a moraine, which can produce anomalously young ages (Stone et al., 2003). We avoided collecting samples from sites which may have been prone to such situations, and we therefore make the assumption that, where we obtained more than one exposure age from the same altitude, the youngest is most likely to represent the time when that site last became ice-free. Therefore we have excluded the ages from samples L7.1.2 (54.4 ka), L7.201.2 (19.7 ka) and L7.2.1 (21.0 ka) from further discussion.

Above 439 m a.s.l., samples from the two sites together record a general trend of decreasing age with decreasing altitude, indicating a progressive decline in surface elevation of the ice sheet with time (Fig. 3a). However, at 411 m a.s.l., an exposure age of 13.9 ka was obtained (sample L7.201.3), which does not fit that trend. Since there is evidence for prior exposure in other samples at this altitude, we regard the exposure age for this sample as only a maximum age for deglaciation. That is, deglaciation could not have occurred any earlier than 13.9 ka, but may have been later. In support of this interpretation, we also note that the sample is slightly embedded in the underlying basaltic scoria, which may indicate deposition during an earlier ice advance.

The ^3He exposure ages of xenolith pyroxenes from 411 m a.s.l. on Overton Peak range from 0 to 35.9 ka (±4 ka; Table 2). These ages are minima as there is likely a small contribution of in situ radiogenic ^4He produced since eruption. One sample yields a ^3He age that significantly pre-dates the LGM. We believe that the age variation is real since that sample (L7.201.1.4) yields ages that reproduce within analytical uncertainty (35.9 ± 3.9 ka and 33.0 ± 2.6 ka).

Discussion

^{10}Be exposure ages

Our dataset of nine ^{10}Be exposure ages is relatively small compared with studies utilizing cosmogenic isotopes from elsewhere in the world. This is largely because our field site, like most others in Antarctica, is remote and difficult to access, and we spent very little time there. Nevertheless, small datasets from Antarctica such as ours are important because the past configuration and rate of thinning since LGM of the Antarctic ice sheet are still not well-known. Here we show that even a limited dataset can contribute to understanding the history of the Alexander Island ice cap.

Altitudinal profiles of surface exposure ages can be used to give information about past ice cap/sheet thickness in addition to ice-sheet thinning trajectories. In the Results section, we explained that we have excluded three samples from our discussion because their exposure ages imply they have experienced multiple periods of exposure and therefore do not reflect timing of the last deglaciation at the sample sites. Excluding those ages, our data suggest a general trend of decreasing ice surface elevation, which here equates to decreasing ice cap thickness, on NW Alexander Island and Rothschild Island

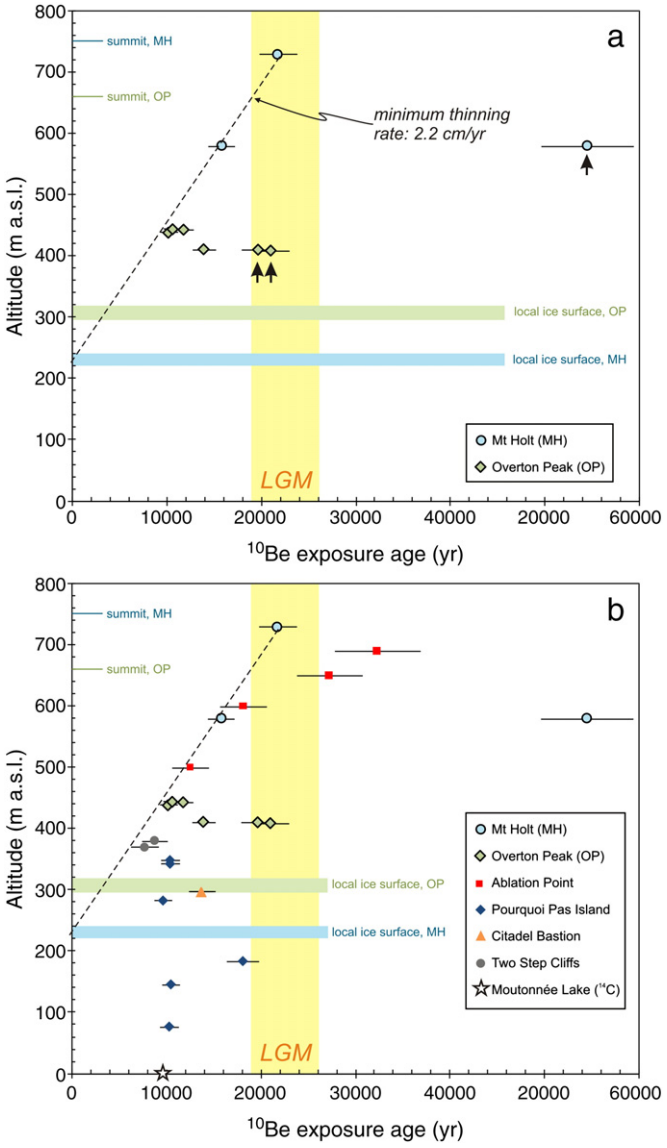

Figure 3. a. ^{10}Be exposure ages versus altitude from Mt Holt (MH) and Overton Peak (OP). Local ice surface elevations were taken from photogrammetry (OP) and ASTER GDEM (MH). The samples marked with upward pointing arrows are those that were excluded from the discussion (see text). The dashed line represents the minimum average thinning rate (2.2 cm/yr) for ice at Mt Holt. The yellow shaded area shows the duration of the last glacial maximum (LGM; 19–26 ka); b. ^{10}Be exposure ages from our study in comparison with others from eastern Alexander Island (Ablation Point and Two Step Cliffs, Bentley et al., 2006; Citadel Bastion, Hodgson et al., 2009) and Marguerite Bay (Pourquoi Pas Island, Bentley et al., 2011). Also shown is a minimum radiocarbon age (calibrated ^{14}C) for deglaciation of Moutonnée Lake (near Ablation Point) from foraminifera in lake sediment (Bentley et al., 2005). The local ice surfaces, summit altitudes and line representing minimum thinning rate are identical to those shown in a.

https://doi.org/10.1016/j.yqres.2011.11.012 Published online by Cambridge University Press

(Fig. 3a). But when did that decrease in surface elevation begin? The answer depends on how we interpret the exposure age from our highest elevation sample, collected from near the summit of Mt Holt (MH). One interpretation is that its exposure age of 21.7 ka ± 2.0 ka is a minimum age for deglaciation. In that case, this site was ice-free by around 21.7 ka. With this interpretation, it is possible that the decrease in ice surface elevation began earlier than 21.7 ka, and that the summit of MH was perhaps ice-free throughout the whole LGM period (19–26 ka). In that case it might have acted as a refuge for biological organisms during the last glacial period (cf. Convey et al., 2008), but not through multiple glacial periods; for that we would expect a much older exposure age. On the other hand, because the 21.7 ka age was obtained from a sample consisting of amalgamated erratic pebbles, we cannot rule out the possibility that its age reflects some inherited ^{10}Be from previous periods of exposure. In that situation, the age should be treated as a maximum for deglaciation, meaning that the site became ice-free only after 21.7 ka.

Our ages from Overton Peak (OP) are limited for showing timing of deglaciation because they fall within a very small altitudinal range. The lowermost three samples are all from the same elevation (~410 m a.s.l.), but have ages ranging from 13.9 to 21.0 ka (Fig. 3a). We have used the youngest age (13.9 ka) as most likely to represent deglaciation, but with the caveat that it might also have had a complex exposure history making it a maximum age. The remaining three ages form a cluster around 11 ka (Fig. 3a), with the youngest at 10.2 ± 0.9 ka. The present ice surface adjacent to OP is 296–318 m a.s.l. (Fig. 3a). Those exposure ages therefore suggest that a maximum of 115 m of thinning has occurred at OP since 10.2 ka. We cannot say when the summit of OP, at 660 m a.s.l., was deglaciated because we did not sample higher than 444 m a.s.l. there due to lack of time at the site. However, since OP is lower than MH, we think it likely that OP deglaciated after MH.

The small size of our datasets from MH and OP inevitably limits the conclusions we can draw from them. Nevertheless, when taken together and with the addition of the present local ice surface elevation, a thinning trajectory for the ice cap on NW Alexander Island and Rothschild Island emerges. If we assume that the ^{10}Be age from the summit of MH represents the time when it became ice-free, we can draw a line connecting that point with the present-day local ice surface elevation at MH to give a possible thinning trajectory for the ice cap since 21.7 ka (Fig. 3a). This line also passes through sample L7.1.1, collected from 580 m a.s.l. on MH, which has an exposure age of 15.8 ± 1.4 ka. The line represents an average ice cap thinning rate of 2.2 cm/yr over the past 21.7 ka. If we use the alternative interpretation that the summit age from MH may be too old and that the site may therefore have become ice-free after 21.7 ka, then 2.2 cm/yr would be only a *minimum* average thinning rate. Some of the exposure ages from OP lie on the line we have drawn for thinning at MH, but at OP we do not have the altitudinal range of samples to test whether thinning there took place at the same rate as at MH. Lowering of the ice surface since 10.2 ka may have occurred episodically at the same rate as at MH, but it could not have been sustained for the whole Holocene period because that would have resulted in a lower ice surface than is presently observed.

As we discussed earlier, sites previously visited on Alexander Island appear to have been submerged by the Alexander Island ice cap (Clapperton and Sugden, 1982; Bentley et al., 2006). Therefore those studies were not able to determine the maximum thickness of the Alexander Island ice cap during the LGM. Our results imply that neither MH nor OP rose above the ice cap during the LGM, and therefore we are also unable to determine maximum ice thickness in that area. Consequently we cannot verify the existing model predictions that fall between at least 1 km maximum thickness and more than 3.5 km (Payne et al., 1989; Denton et al., 1991; Huybrechts, 2002). Nevertheless, our data allow us to make a minimum estimate of ice thickness. For this, we compared the past ice surface elevations at the LGM derived from our exposure ages with measured present-day ice elevations. Our exposure ages suggest that ice cover on MH was at least 490 m thicker during the LGM period than at present (ice surface elevation on the eastern side of MH is 230 ± 10 m a.s.l. today; Fig. 3a). Our data from OP do not allow us to estimate ice thickness at the LGM, but they show that, at 10.2 ka, the ice cap there was at least 115 m thicker than present.

To put our ^{10}Be exposure ages from NW Alexander Island in a wider context, we have shown them alongside published ages from eastern Alexander Island (Bentley et al., 2006; Hodgson et al., 2009) and Marguerite Bay (Bentley et al., 2011) (Fig. 3b). Whichever interpretation of the summit age of MH one chooses to accept, our data suggest more rapid thinning of the ice cap between the LGM and ~10 ka in the NW of Alexander Island than in the east. However, our sample sites are more than 200 km away from those of eastern Alexander Island (Fig. 1) so we are cautious about drawing direct comparisons.

Existing data from Marguerite Bay to the north of Alexander Island (see exposure ages from Pourquoi Pas Island, Fig. 3b; Bentley et al., 2011) indicate that ice thinned very rapidly to reach its present-day limits around 10 ka at that location. Whilst our data do not preclude the possibility that the ice cap thinned beyond 10 ka, none of our exposure ages are younger than 10.2 ka so we can only speculate what happened after that time. However, it is conceivable that rapid thinning and retreat of ice from the inner shelf of Marguerite Bay around 10 ka could have influenced the timing and rate of deglaciation of northern Alexander Island. In the absence of exposure ages from lower elevations in NW Alexander Island, only a better-constrained deglacial history for the continental shelf to the west of Alexander Island would indicate how the ice cap on NW Alexander Island might have behaved during the Holocene. Age control similar to that obtained for Marguerite Trough Ice Stream is needed (Ó Cofaigh et al., 2005; Kilfeather et al., 2011).

^{3}He exposure ages

Contrary to our expectation, the ^{3}He ages from our xenoliths suggest an exposure age range of 0–36 ka for a single site at 411 m a.s.l. on Overton Peak (OP). ^{10}Be exposure ages of 13.9 and 19.7 ka were obtained from erratics at the same site (L7.201.3 and L7.201.2), although we interpret those samples as having a complex exposure history (the thinning trend exhibited by our other data suggests deglaciation occurred later than 13.9 ka at this elevation). We therefore suggest that the range in ^{3}He ages reflects variation in the timing of xenolith exhumation (and possibly burial) due to periglacial processes. We envisage these processes as relatively small-scale and assume that they have not overturned or buried the larger erratic cobbles lying on the bedrock regolith surface. We were not aware of the presence of patterned ground and stripes formed by periglacial creep processes during our field campaign, but they are visible in an aerial photo of OP which was taken the following season (Figs. 2c and d). The old ^{3}He age of 36 ka probably reflects additional exposure at this site during an ice-free period (or periods) prior to the LGM; this would not be surprising since the host basalt for the xenoliths was erupted at 5.4 Ma.

Relevance to ice sheet models

In its fourth assessment report, the Intergovermental Panel on Climate Change stated that models used for sea level predictions 'do not include the full effects of changes in ice sheet flow, because a basis in published literature is lacking' (IPCC, 2007). Models that seek to predict future changes in mass of the ice sheets must incorporate long-term responses of those ice sheets to climatic change. They therefore require observational data on the past configuration of those ice sheets (Bentley, 2010). We liken our study to one tiny piece in a

https://doi.org/10.1016/j.yqres.2011.11.012 Published online by Cambridge University Press

very large jigsaw – for a very small part of Antarctica, we have provided first constraints on ice sheet thinning rates, and to a limited extent, the timing of ice surface lowering. Prior to this, little was known about how this part of the Alexander Island ice cap had responded to climatic warming since the LGM.

Conclusions

1. Assuming no prior exposure, our ^{10}Be exposure ages suggest that the ice cap on NW Alexander Island thinned from at least 21.7 ka until 10.2 ka, through at least part of the LGM, and at an average rate of 2.2 cm/yr. However, we cannot rule out the possibility that the 21.7 ka age may be too old (due to inherited ^{10}Be from prior exposure) to represent the timing of the last deglaciation at Mt Holt. In that situation, the average thinning rate of the ice cap would have been greater than 2.2 cm/yr.
2. The data provide a minimum estimate suggesting that the thickness of the ice cap on NW Alexander Island during the LGM was at least 490 m thicker than present. We are unable to give a maximum paleo-ice thickness, and therefore cannot verify model predictions of 1–3.5 km projected by others, because neither site we visited rises high enough to record the upper limit of the ice.
3. We report the first constraints on rate and timing of thinning of the ice cap on NW Alexander Island. However, more exposure ages from altitudes below 400 m a.s.l. and/or better constraints on the deglacial history of the continental shelf to the west of Alexander Island are needed to determine the Holocene ice cap history of this area.

Acknowledgments

We thank the Captain, Officers and crew of HMS Endurance, and BAS field assistants Mark Gorin and Roger Stilwell for their support during Antarctic fieldwork. BAS technicians Mike Tabecki and Hilary Blagbrough crushed the rock samples, Adrian Fox provided aerial photographs, and Lydia Gibson (University of Cambridge) donated the mantle xenoliths from her PhD project. The work was performed in part under the auspices of the US Department of Energy by Lawrence Livermore National Laboratory under contract DE-AC52-07NA27344. This paper is the result of a collaborative study between the British Geological Survey and the British Antarctic Survey as part of the BAS 'Polar Science for Planet Earth' programme, funded by the Natural Environment Research Council. The work was also supported by an Antarctic Science Ltd Bursary to JSJ. We thank Jim Knox, Alan Gillespie, Adam Lewis and an anonymous reviewer for their constructive comments.

Appendix A. Supplementary data

Supplementary data to this article can be found online at doi:10.1016/j.yqres.2011.11.012.

References

Anderson, J.B., Shipp, S.S., Lowe, A.L., Wellner, J.S., Mosola, A.B., 2002. The Antarctic ice sheet during the last glacial maximum and its subsequent retreat history: a review. Quaternary Science Reviews 22, 49–70.

Balco, G., Stone, J.O., Lifton, N.A., Dunai, T.J., 2008. A complete and easily accessible means of calculating surface exposure ages or erosion rates from ^{10}Be and ^{26}Al measurements. Quaternary Geochronology 3, 174–195.

Bentley, M.J., 2010. The Antarctic palaeo record and its role in improving predictions of future Antarctic Ice Sheet change. Journal of Quaternary Science 25, 5–18.

Bentley, M.J., Anderson, J.B., 1998. Glacial and marine geological evidence for the ice sheet configuration in the Weddell Sea–Antarctic Peninsula region during the Last Glacial Maximum. Antarctic Science 10, 307–323.

Bentley, M.J., Hodgson, D.A., Sugden, D.A., Roberts, S.J., Smith, J.A., Leng, M.J., Bryant, C., 2005. Early Holocene retreat of George VI Ice Shelf, Antarctic Peninsula. Geology 33, 173–176.

Bentley, M.J., Fogwill, C.J., Kubik, P.W., Sugden, D.E., 2006. Geomorphological evidence and cosmogenic ^{10}Be/^{26}Al exposure ages for the Last Glacial Maximum and deglaciation of the Antarctic Peninsula Ice Sheet. Geological Society of America Bulletin 118, 1149–1159.

Bentley, M.J., Johnson, J.S., Hodgson, D.A., Dunai, T.J., Freeman, S.P.H.T., Ó'Cofaigh, C., 2011. Rapid deglaciation of Marguerite Bay, western Antarctic Peninsula in the Early Holocene. Quaternary Science Reviews 30, 3338–3349.

Bierman, P.R., Marsella, K.A., Patterson, C., Davis, P.T., Caffee, M., 1999. Mid-Pleistocene cosmogenic minimum-age limits for pre-Wisconsinan glacial surfaces in southwestern Minnesota and southern Baffin Island: a multiple nuclide approach. Geomorphology 27, 25–39.

Bolmer, S.T., 2008. A note on the development of the bathymetry of the continental margin west of the Antarctic Peninsula from 65° to 71°S and 65° to 78°W. Deep-Sea Research II 55, 271–276.

Bruno, L.A., Baur, H., Graf, T., Schlüchter, C., Signer, P., Wieler, R., 1997. Dating of Sirius Group tillites in the Antarctic Dry Valleys with cosmogenic ^{3}He and ^{21}Ne. Earth and Planetary Science Letters 147, 37–54.

Burn, R.W., 1984. The geology of the LeMay Group, Alexander Island. British Antarctic Survey Scientific Reports, 109.

Care, B.W., 1983. The petrology of the Rouen Mountains, northern Alexander Island. British Antarctic Survey Bulletin 52, 63–86.

Clapperton, C.M., Sugden, D.E., 1982. Late Quaternary glacial history of George VI Sound area, West Antarctica. Quaternary Research 18, 243–267.

Clark, P.U., Dyke, A.S., Shakun, J.D., Carlson, A.E., Clark, J., Wohlfarth, B., Mitrovica, J.X., Hostetler, S.W., McCabe, A.M., 2009. The Last Glacial Maximum. Science 325, 710–714.

Convey, P., Gibson, J.A.E., Hillenbrand, C.-D., Hodgson, D.A., Pugh, P.J.A., Smellie, J.L., Stevens, M.I., 2008. Antarctic terrestrial life — challenging the history of the frozen continent? Biological Reviews 83, 103–117.

Cook, A.J., Fox, A.J., Vaughan, D.G., Ferrigno, J.G., 2005. Retreating glacier fronts on the Antarctic Peninsula over the last half century. Science 308, 541–544.

Denton, G.H., Prentice, M.L., Burckle, L.H., 1991. Cainozoic history of the Antarctic Ice Sheet. In: Tingley, R.J. (Ed.), The Geology of Antarctica. Oxford University Press, Oxford, pp. 265–433.

Goehring, B.M., Kurz, M.D., Balco, G., Schaefer, J.M., Licciardi, J., Lifton, N., 2010. A reevaluation of *in situ* cosmogenic ^{3}He production rates. Quaternary Geochronology 5, 410–418.

Graham, A.G.C., Nitsche, F.O., Larter, R.D., 2010. An improved bathymetry compilation for the Bellingshausen Sea, Antarctica, to inform ice-sheet and ocean models. The Cryosphere Discussions 4, 2079–2101. doi:10.5194/tcd-4-2079-2010.

Heroy, D.C., Anderson, J.B., 2007. Radiocarbon constraints on Antarctic Peninsula Ice Sheet retreat following the Last Glacial Maximum (LGM). Quaternary Science Reviews 26, 3286–3297.

Hodgson, D.A., Bentley, M.J., Roberts, S.J., Smith, J.A., Sugden, D.E., Domack, E.W., 2006. Examining Holocene stability of Antarctic Peninsula ice shelves. EOS Transactions, American Geophysical Union 87 (31), 305–308.

Hodgson, D.A., Roberts, S.J., Bentley, M.J., Smith, J.A., Johnson, J.S., Verleyen, E., Vyverman, W., Hodson, A.J., Leng, M.J., Cziferszky, A., Fox, A.J., Sanderson, D.C.W., 2009. Exploring former subglacial Hodgson Lake, Antarctica. Paper I: site description, geomorphology and limnology. Quaternary Science Reviews 28, 2295–2309.

Huybrechts, P., 2002. Sea-level changes at the LGM from ice-dynamic reconstructions of the Greenland and Antarctic ice sheets during the glacial cycles. Quaternary Science Reviews 21, 203–231.

IPCC, 2007. Climate Change 2007: the Physical Science Basis. Contribution of Working Group 1 to the Fourth Assessment Report of the Intergovernmental Panel on Climate Change. Cambridge University Press, UK.

Johnson, J.S., Smellie, J.L., Nelson, A.E., Stuart, F.M., 2009. History of the Antarctic Peninsula Ice Sheet since the early Pliocene—evidence from cosmogenic dating of Pliocene lavas on James Ross Island, Antarctica. Global and Planetary Change 69, 205–213.

Johnson, J.S., Bentley, M.J., Roberts, S.J., Binnie, S.A., Freeman, S.P.H.T., 2011. Holocene deglacial history of the north east Antarctic Peninsula - a review and new chronological constraints. Quaternary Science Reviews 30, 3791–3802. doi:10.1016/j.quascirev.2011.10.011.

Kennedy, D.S., Anderson, J.B., 1989. Glacial–marine sedimentation and Quaternary glacial history of Marguerite Bay, Antarctic Peninsula. Quaternary Research 31, 255–276.

Kilfeather, A.A., Ó Cofaigh, C., Lloyd, J.M., Dowdeswell, J.A., Xu, S., Moreton, S.G., 2011. Ice-stream retreat and ice-shelf history in Marguerite Trough, Antarctic Peninsula: sedimentological and foraminiferal signatures. Geological Society of America, Bulletin 123 (5/6), 997–1015. doi:10.1130/B30282.1.

Lal, D., 1991. Cosmic ray labeling of erosion surfaces: in situ nuclide production rates and erosion models. Earth and Planetary Science Letters 104 (2–4), 424–439.

Larter, R.D., Cunningham, A.P., 1993. The depositional pattern and distribution of glacial-interglacial sequences on the Antarctic Peninsula Pacific margin. Marine Geology 109, 203–219.

Nishiizumi, K., Kohl, C.P., Arnold, J.R., Klein, J., Fink, D., 1991. Cosmic ray produced ^{10}Be and ^{26}Al in Antarctic rocks: exposure and erosion rates. Earth and Planetary Science Letters 104, 440–454.

Nishiizumi, K., Imamura, M., Caffee, M.W., Southon, J.R., Finkel, R.C., McAninch, J., 2007. Absolute calibration of ^{10}Be AMS standards. Nuclear Instruments and Methods in Physics Research Section B: Beam Interactions with Materials and Atoms 258 (2), 403–413.

Ó Cofaigh, C., Pudsey, C.J., Dowdeswell, J.A., Morris, P., 2002. Evolution of subglacial bedforms along a paleo-ice stream, Antarctic Peninsula continental shelf. Geophysical Research Letters 29. doi:10.1029/2001GL014488.

Ó Cofaigh, C., Dowdeswell, J.A., Allen, C.S., Hiemstra, J., Pudsey, C.J., Evans, J., Evans, D.J.A., 2005. Flow dynamics and till genesis associated with a marine-based Antarctic palaeo-ice stream. Quaternary Science Reviews 24, 709–740.

Payne, A.J., Sugden, D.A., Clapperton, C.M., 1989. Modeling the growth and decay of the Antarctic Peninsula Ice Sheet. Quaternary Research 31, 119–134.

Pope, P.G., Anderson, J.B., 1992. Late Quaternary glacial history of the northern Antarctic Peninsula's western continental shelf: evidence from the marine record. In: Elliot, D.H. (Ed.), Contributions to Antarctic Research III: Antarctic Research Series, 57, pp. 63–91.
Pritchard, H.D., Arthern, R.J., Vaughan, D.G., Edwards, L.A., 2009. Extensive dynamic thinning on the margins of the Greenland and Antarctic ice sheets. Nature 461, 971–975.
Roberts, S.J., Hodgson, D.A., Bentley, M.J., Sanderson, D.C.W., Milne, G., Smith, J.A., Verleyen, E., Balbo, A., 2009. Holocene relative sea-level change and deglaciation on Alexander Island, Antarctic Peninsula, from elevated lake deltas. Geomorphology 112, 122–134.
Smellie, J.L., Pankhurst, R.J., Hole, M.J., Thomson, J.W., 1988. Age, distribution and eruptive conditions of late Cenozoic alkaline volcanism in the Antarctic Peninsula and eastern Ellsworth Land: review. British Antarctic Survey Bulletin 80, 21–49.
Smith, J.A., Bentley, M.J., Hodgson, D.A., Roberts, S.J., Leng, M.J., Lloyd, J.M., Barrett, M.S., Bryant, C., Sugden, D.E., 2007. Oceanic and atmospheric forcing of early Holocene ice shelf retreat, George VI Ice Shelf, Antarctica Peninsula. Quaternary Science Reviews 26, 500–516.
Stone, J.O., 2000. Air pressure and cosmogenic isotope production. Journal of Geophysical Research 105 (B10), 23753–23759.
Stone, J.O., Balco, G., Sugden, D.E., Caffee, M.W., Sass, L.C., Cowdery, S.G., Siddoway, C., 2003. Holocene deglaciation of Marie Byrd Land, West Antarctica. Science 299, 99–102.
Sugden, D.A., Bentley, M.J., Ó Cofaigh, C., 2006. Geological and geomorphological insights into Antarctic ice sheet evolution. Philosophical Transactions of the Royal Society A 364, 1607–1625.
Summerfield, M.A., Stuart, F.M., Cockburn, H.A.P., Sugden, D.E., Denton, G., Dunai, T., Marchant, D.R., 1999. Long-term rates of denudation in the Dry Valleys, Transantarctic Mountains, southern Victoria Land, Antarctica based on in-situ-produced cosmogenic ^{21}Ne. Geomorphology 27, 113–129.

https://doi.org/10.1016/j.yqres.2011.11.012 Published online by Cambridge University Press